A Cross-correlation method to search for gravitational wave bursts with AURIGA and Virgo

THE AURIGA COLLABORATION

M. Bignotto[1,2], M. Bonaldi[3,4], M. Camarda[5] , M. Cerdonio[1,2], L. Conti[1,2], M. Drago[1,2], P. Falferi[3,4], N. Liguori[1,2], S. Longo[6], R. Mezzena[4,7], A. Mion[4,7], A. Ortolan[6], G.A. Prodi[4,7], V. Re[4,7], F. Salemi[4,7], L. Taffarello[2], G. Vedovato[2], A. Vinante[3,4], S. Vitale[4,7], J.P. Zendri[2]

[1] Dipartimento di Fisica, Università di Padova, Via Marzolo 8, 35131 Padova, Italy
[2] INFN, Sezione di Padova, Via Marzolo 8, 35131 Padova, Italy
[3] Istituto di Fotonica e Nanotecnologie, CNR-Fondazione Bruno Kessler, I-38050 Povo (Trento), Italy
[4] INFN, Gruppo Collegato di Trento, Sezione di Padova, I-38050 Povo, Trento, Italy
[5] Dipartimento di Ingegneria Informatica, Università di Padova, Via G. Gradenigo 6a, 35131 Padova, Italy
[6] INFN, Laboratori Nazionali di Legnaro, 35020 Legnaro, Padova, Italy
[7] Dipartimento di Fisica, Università di Trento, I-38050 Povo, Trento, Italy

THE Virgo COLLABORATION

F.Acernese [7,9], M.Alshourbagy[15,16], P.Amico[13,14], F.Antonucci[19], S.Aoudia[10], P.Astone[19], S.Avino[7,8], L.Baggio[1], G.Ballardin[2], F.Barone[7,9], L.Barsotti[15,16], M.Barsuglia[11], Th.S.Bauer[21], S.Bigotta[15,16], S.Birindelli[15,16], C.Boccara[12], F.Bondu[10], L.Bosi[13], S.Braccini [15], C.Bradaschia[15], A.Brillet[10], V.Brisson[11], D.Buskulic[1], G.Cagnoli[3], E.Calloni[7,8], E.Campagna[3,5], F.Carbognani[2], F.Cavalier[11], R.Cavalieri[2], G.Cella[15], E.Cesarini[3,4], E.Chassande-Mottin[10], A.-C.Clapson[11], F.Cleva[10], E.Coccia[23,24], C.Corda[15,16], A.Corsi[19], F.Cottone[13,14], J.-P.Coulon[10], E.Cuoco[2], S.D'Antonio[23], A.Dari[13,14], V.Dattilo[2], M.Davier[11], R.De Rosa[7,8], M.Del Prete [15,17], L.Di Fiore[7], A.Di Lieto[15,16], M.Di Paolo Emilio[23,25], A.Di Virgilio[15], M.Evans[2], V.Fafone[23,24], I.Ferrante[15,16], F.Fidecaro[15,16], I.Fiori[2], R.Flaminio[6], J.-D.Fournier[10], S.Frasca [19,20], F.Frasconi [15], L.Gammaitoni[13,14], F.Garufi [7,8], E.Genin[2], A.Gennai[15], A.Giazotto[2,15], L.Giordano[7,8], V.Granata[1], C.Greverie[10], D.Grosjean[1], G.Guidi[3,5], S.Hamdani[2], S.Hebri [2], H.Heitmann[10], P.Hello[11], D.Huet[2], S.Kreckelbergh[11], P.La Penna [2], M.Laval[10],

N.Leroy [11], **N.Letendre**[1], **B.Lopez**[2], **M.Lorenzini**[3,4], **V.Loriette**[12],
G.Losurdo[3], **J.-M.Mackowski**[6], **E.Majorana**[19], **C.N.Man**[10],
M.Mantovani[17,16], **F.Marchesoni**[13,14], **F.Marion**[1], **J.Marque**[2],
F.Martelli[3,5], **A.Masserot**[1], **F.Menzinger**[2], **L.Milano**[7,8],
Y.Minenkov[23], **C.Moins**[2], **J.Moreau**[12], **N.Morgado**[6], **S.Mosca**[7,8],
B.Mours[1], **I.Neri**[13,14], **F.Nocera**[2], **G.Pagliaroli**[23], **C.Palomba**[19],
F.Paoletti [2,15], **S.Pardi**[7,8], **A.Pasqualetti**[2], **R.Passaquieti**[15,16],
D.Passuello[15], **F.Piergiovanni**[3,5], **L.Pinard**[6], **R.Poggiani**[15,16],
M.Punturo[13], **P.Puppo**[19], **P.Rapagnani**[19,20], **T.Regimbau** [10],
A.Remillieux[6], **F.Ricci** [19,20], **I.Ricciardi**[7,8], **A.Rocchi**[23],
L.Rolland[1], **R.Romano**[7,9], **P.Ruggi**[2], **G.Russo**[7,8], **S.Solimeno**[7,8],
A.Spallicci[10], **B.L.Swinkels**[2], **M.Tarallo**[15,16], **R.Terenzi**[23],
A.Toncelli[15,16], **M.Tonelli**[15,16], **E.Tournefier**[1], **F.Travasso**[13,14],
G.Vajente [18,16], **J.F.J. van den Brand**[21,22], **S. van der Putten**[21],
D.Verkindt[1], **F.Vetrano**[3,5], **A.Viceré**[3,5], **J.-Y.Vinet** [10], **H.Vocca**[13],
M.Yvert[1]

[1]Laboratoire d'Annecy-le-Vieux de Physique des Particules (LAPP), IN2P3/CNRS, Université de Savoie, Annecy-le-Vieux, France
[2]European Gravitational Observatory (EGO), Cascina (Pi), Italia.
[3]INFN, Sezione di Firenze, Sesto Fiorentino, Italia.
[4] Università degli Studi di Firenze, Firenze, Italia.
[5] Università degli Studi di Urbino "Carlo Bo", Urbino, Italia.
[6]LMA, Villeurbanne, Lyon, France.
[7] INFN, sezione di Napoli, Italia.
[8] Università di Napoli "Federico II" Complesso Universitario di Monte S.Angelo, Italia.
[9] Università di Salerno, Fisciano (Sa), Italia.
[10]Departement Artemis – Observatoire de la Côte d'Azur, BP 4229 06304 Nice, Cedex 4, France.
[11]LAL, Univ Paris-Sud, IN2P3/CNRS, Orsay, France.
[12]ESPCI, Paris, France.
[13]INFN, Sezione di Perugia, Italia.
[14]Università di Perugia, Perugia, Italia.
[15]INFN, Sezione di Pisa, Italia.
[16] Università di Pisa, Pisa, Italia.
[17] Università di Siena, Siena, Italia.
[18] Scuola Normale Superiore, Pisa, Italia.
[19]INFN, Sezione di Roma, Italia.
[20]Università "La Sapienza", Roma, Italia
[21]National institute for subatomic physics, NL-1009 DB Amsterdam, The Netherlands.
[22]Vrije Universiteit, NL-1081 HV Amsterdam, The Netherlands.
[23]INFN, Sezione di Roma Tor Vergata, Roma, Italia.
[24] Università di Roma Tor Vergata, Roma, Italia.
[25] Università dell'Aquila, L'Aquila, Italia.

e-mail virginia.re@lnl.infn.it

Abstract.
We present a method to search for transient gravitational waves using a network of detectors with different spectral and directional sensitivities: the interferometer Virgo and the bar detector AURIGA. The data analysis method is based on the measurements of the correlated energy in the network by means of a weighted cross-correlation. To limit the computational load, this coherent analysis step is performed around time-frequency coincident triggers selected by an excess power event trigger generator tuned at low thresholds. The final selection of gravitational wave candidates is performed by a combined cut on the correlated energy and on the significance as measured by the event trigger generator. The method has been tested on one day of data of AURIGA and Virgo during September 2005. The outcomes are compared to the results of a stand-alone time-frequency coincidence search. We discuss the advantages and the limits of this approach, in view of a possible future joint search between AURIGA and one interferometric detector.

1. Introduction

We present a study on the performances of a gravitational wave (GW) observatory composed of a hybrid network of detectors. In particular, we focus on the possibility to use a resonant detector to perform GW observations with one interferometric detector.

Our case study consists in 24 hours of joint observations between AURIGA and Virgo on September 15,2005. Similar joint searches could be of interest for the period after the fifth LIGO scientific run (S5) and the first Virgo science run (VSR1), when most of the interferometers will be shut down for upgrading. Current plans are that GEO-600 will be kept in operation until the start of the sixth LIGO and of the second Virgo science runs (S6 and VSR2 respectively), supported by the LIGO Hanford 2k detector over weekends [1].

In the past years, various searches for GW signals have been independently performed by networks of resonant bars [2, 3, 4] or interferometers [5, 6]. There have been also some attempts to perform burst searches among detectors with different spectral sensitivity and orientation: by TAMA ([8]) and the LIGO Scientific Collaboration (LSC [7]) [9], by AURIGA and the LSC [10, 11, 12] and by the INFN bars and the Virgo Collaboration [14].

The proposed network search strategy takes as a starting point the Wave-Burst+CorrPower [15, 16] search used by LSC for the S3 and S4 analyses [17, 6]. That search was greatly innovative: a two-step search composed of an ExcessPower-like event trigger generator plus a cross-correlation test which allowed an efficient reduction of false alarms. In that case, however, the detectors partecipating to the network were almost aligned and had a similar spectral sensitivity. An extension of such methodology to the case of similar but misaligned detectors has been discussed in literature [18]. Our work presents a further generalization to detectors with different spectral sensitivities, so that it can be implemented between a resonant bar and an interferometer. To better charac-terize the method, we compare its performances with those of a simple time-frequency

coincidence search.

The paper is organized as follows: in section 2 we introduce the search method. Section 3 presents an overview of the exchanged data and summarizes the main steps of the network pipeline and of the tuning performed on chosen test-statistics. Results and conclusions are presented in section 4 and 5 respectively.

2. The search method

The GW search method described in this paper has two components: the event trigger generator, whose role is to select a subset of *interesting* triggers and a coherent analysis. The trigger search is based on Waveburst [19], an excess power algorithm that uses the wavelet decomposition. In the present work, Waveburst has been run in coincidence mode, i.e. the algorithm selects time-frequency coincident excesses of power between the two detectors. The coherent follow-up of coincident events is based on a cross-correlation test between data streams weighted by a combination of the strain sensitivities of the two detectors (XCorr).

Our method assumes that the GW polarization components in the wavefront frame, $h_+(t)$ and $h_\times(t)$, can be parametrized as

$$h_+(t) = h_0(t) \cdot \cos[\psi(t)] \qquad h_\times(t) = \epsilon \cdot h_0(t) \cdot \sin[\psi(t)] \tag{1}$$

where $h_0(t)$ and $\psi(t)$ are time-varying amplitude and phase, common to both polarization components, and ϵ is the ratio of cross and plus amplitudes. A large class of GW signals can be parametrized as described above, including linearly, elliptically and circularly polarized GWs, even with sweeping frequencies.

The strain produced on the detector α by an incoming burst signal is:

$$h_\alpha(t) = F_{\alpha+}(\theta, \phi) \cdot h_+(t) + F_{\alpha\times}(\theta, \phi) \cdot h_\times(t) \tag{2}$$

where $F_{\alpha+}$ and $F_{\alpha\times}$ are the *antenna pattern* functions and (θ, ϕ) is the location of the GW source (see [13] and references therein). Following [20], eq.2 becomes:

$$h_\alpha(t) = h_0(t) \cdot R_\alpha(\theta, \phi, \epsilon) \cdot \cos[\psi(t) + \xi_\alpha(\theta, \phi, \epsilon)] \tag{3}$$

where R_α is a directional sensitivity, ξ_α is a phase shift ‡. The reconstructed strain at the input of detector α is $x_\alpha(t) = h_\alpha(t) + n_\alpha(t)$, where n_α is the detector noise, independent among different detectors. It has been shown in [21] that the following linear combination of the two reconstructed strains, called *null stream*, cancels the signal: $x_{\texttt{null}}(t) \equiv x_1(t)R_2 - x_2(t + t')R_1$, where t' includes the light travel time and a suitable fraction of the typical GW period, so that $\psi(t) + \xi_1 = \psi(t + t') + \xi_2$§.

---

‡ With some algebra, it is easy to find that $R_\alpha = \sqrt{(F_{\alpha+})^2 + (F_{\alpha\times} \cdot \epsilon)^2}$ and $\xi_\alpha = -\texttt{arctan}[\frac{F_{\alpha\times} \cdot \epsilon}{F_{\alpha+}}]$.
§ An additional assumption is required here: the envelope of the GW signal be smooth in time so that $h_0(t) \simeq h_0(t + t')$. Whenever one considers a cross-correlation with a narrow-band detector, this approximation is automatically verified since the reconstructed strain at input has to be bandlimited by a suitable filter (see fig.1).

The resulting noise power spectrum of the null stream is very colored, showing a variance per unit bandwidth $\sigma_{null}^2(f) = S_{h1}(f)R_2^2 + S_{h2}(f)R_1^2$, where $S_{h\alpha}$ are the one sided noise power spectral densities of the detectors in terms of GW strain. We take this into account in the coherent analysis by considering a weighted null stream, normalized by its variance , $x_{\texttt{null},w}(t) \equiv x_{1,w}(t)R_2 - x_{2,w}(t+t')R_1$, where $x_{\alpha,w}(t)$ are weighetd reconstructed strains whose Fourier transforms are given by

$$\widetilde{x}_{\alpha,w}(f) = \frac{\widetilde{x}_\alpha(f)}{\sigma_{\texttt{null}}(f)} = \frac{\widetilde{x}_\alpha(f)}{\sqrt{S_1(f)R_2^2 + S_2(f)R_1^2}} \tag{4}$$

where $S_{1,2}$ are the noise power spectral densities of the detectors in terms of GW strain. Hence, the normalized null stream is $x_{\texttt{null},w}(t) \equiv x_{1,w}(t)R_2 - x_{2,w}(t+t')R_1$.

One well known method to search for GW signals in the data relies on the minimization of the null energy [20, 21], $E_{\texttt{null}} \equiv \int dt\, x_{\texttt{null},w}^2(t)$, where the time integral is performed on the signal duration plus any typical response time of the narrower band detector. The null energy can be expressed in terms of the correlated energy and the incoherent energy of the network: $E_{\texttt{null}} = -E_{\texttt{cor}} + E_{\texttt{inc}}$. The former is the contribution of the cross-correlation of the detectors, $E_{\texttt{cor}} = 2 \int dt\, x_{1,w}(t)x_{2,w}(t+t')R_1R_2$. The latter is the auto-correlation contribution of the detectors, $E_{\texttt{inc}} = \int dt(x_1^2(t)R_2^2 + x_2^2(t+t')R_1^2)$. As discussed in [21], a GW candidate is selected against background events more efficiently by maximizing $E_{\texttt{cor}}$ rather than by minimizing $E_{\texttt{null}}$. In fact, $E_{\texttt{null}}$ can take low values even for accidental events with small $E_{\texttt{cor}}$ and $E_{\texttt{inc}}$; instead, for detectable GW signals, we expect a higher $E_{\texttt{inc}}$, almost balanced by a positive $E_{\texttt{cor}}$. For these reasons, this coherent step of network analysis is based on the maximization of the correlated energy $E_{\texttt{cor}}$ in our null stream.

In principle, $E_{\texttt{cor}}$ depends on θ, ϕ and ϵ of the source through t', R_1 and R_2. However, we checked that in the case of random polarized GW radiation, emitted by sources distributed either in the galaxy or uniformly in the sky, we can follow an approximate maximization procedure of $E_{\texttt{cor}}$ assuming $R_1 \simeq R_2$ and therefore maximizing only on the parameters t and t' . The main reason is that AURIGA is limiting the common bandwidth and at the same time shows a worse strain power spectral density; therefore, the $\sigma_{\texttt{null}}(f)$ defined in eq.4 is dominated by the strain noise of AURIGA unless $R_{AU}/R_V \gg 1$. This condition however is occurring rarely enough: $R_{AU}/R_V < 2.4$ with 90 % probability for a galactic population of sources, and very similar values occur also considering the LIGO or GEO-600 interferometers in place of Virgo. Fig.1 shows the $\sigma_{\texttt{null}}(f)$, corresponding to $R_{AU}/R_V = \{0, 1, 2.4\}$. These curves are quite similar and therefore it is advisable to approximate $R_1 = R_2$ in eq.4 and in the above definitions of $E_{\texttt{cor}}$, i.e. to compute the cross correlation on filtered data streams:

$$\widetilde{x}'_{1,w}(f) \equiv \frac{\widetilde{x}_1}{\sqrt{S_1(f) + S_2(f)}} \qquad\qquad \widetilde{x}'_{2,w}(f) \equiv \frac{\widetilde{x}_2}{\sqrt{S_1(f) + S_2(f)}} \tag{5}$$

Moreover, to be robust against noise fluctuations and relative calibration errors between AURIGA and Virgo, we considered the r-statistic of such filtered data streams

in place of the E_{cor}:

$$r_{1,2} \equiv \frac{\int dt x'_{1,w}(t) x'_{2,w}(t+t')}{\sqrt{\int d\tau x'^2_{1,w}(t) \int d\tau x'^2_{2,w}(t)}} \tag{6}$$

where we integrate over a time window of fixed duration and search for local maxima as a function of the time t and time shift t' between the data streams ‖.
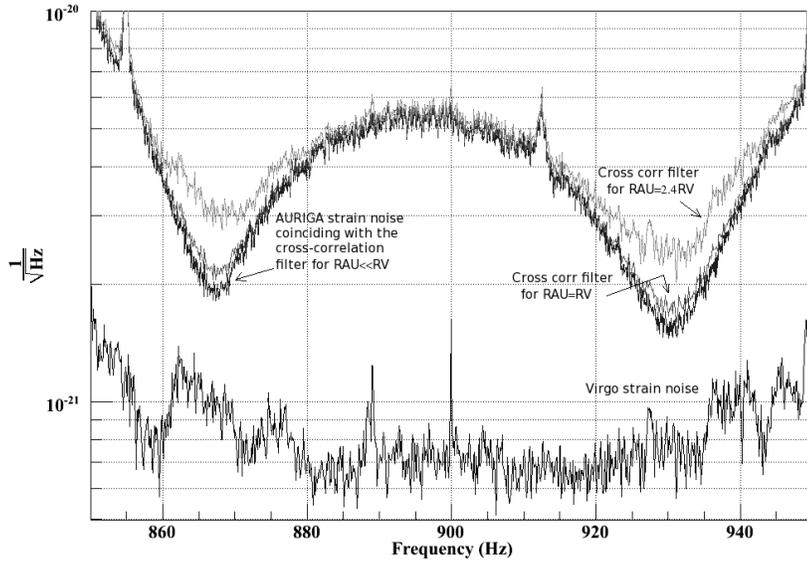

Figure 1: Strain noise power spectral densities of Virgo and AURIGA detectors on September 15, 2005 (respectively first and second black continuous lines from the bottom of the figure) and the spectral filters for different ratios R_{AU}/R_V. The lower limit for such filter,corresponding to sources with $R_{AU} \ll R_V$, coincides with the AURIGA strain noise. The dark gray curve (nearly superimposed to the AURIGA spectrum) shows the filter $\sigma_{\text{null}}(f)$ with the approximation $R_{AU} = R_V$. The light gray curve shows the exact spectral filter for sources with $R_{AU} = 2.4R_V$ and can be interpreted as an upper limiting curve: in fact we find that $R_{AU} \leq 2.4R_V$ with 90% probability for a source distributed in the Milky Way with random polarization. We conclude that the spectral filter with $R_{AU} = R_V$ is a satisfactory approximation for our purposes.

3. Network Analysis

We analyzed the 24 hours of data starting from UTC time 14 Sep 2005 23:11:27. In this time period, Virgo was performing its seventh commissioning run (C7) while AURIGA was in stable operation. The common observation time is reduced to 16 hours and 33 minutes, taking into account the periods when the Virgo interferometer was not in scientific data taking. Moreover, the Virgo Collaboration provided a list of vetoes to

‖ At the end, the main difference with respect to the Corr-Power coherent followup adopted by LIGO is the use of the spectral filter.

flag the most noisy periods, corresponding to a further 14.5% reduction of the live time. The S_h sensitivity curves for the two detectors in the $[850 \div 950]$ Hz band on September 15 are shown in fig.1.

3.1. Pipeline description

Fig.2 shows the pipeline: as a first step, raw data from the two detectors are whitened and bandpassed to match the AURIGA bandwidth (i.e. 850 - 950 Hz), then they are fed in as input to WaveBurst [19].

WaveBurst has been configured to search for coincident excesses of power on the two data sets over 4 wavelet decomposition levels, corresponding to time/frequency resolutions ranging from 4.916 ms by 101.72 Hz to 39.32 ms by 12.72 Hz. It then produces the list of triggers, containing all the trigger parameters (e.g. the central time in GPS seconds, the central frequency, the frequency range, the geometric significance, Z¶, the Signal to Noise Ratio, SNR, etc.). For each of those events, the last step of the pipeline, XCorr, selects the corresponding segments of weighted filtered data (see sec. 2) and, by sliding on t and t' the two time series [+], it searches the maximum of the cross-correlation coefficient, r , computed over a given time window.

Within our approach, similarly to what has been used in [6], Z and r are the main test statistics which characterize each event at the output of the pipeline. A combined threshold on these quantities sets the overall false alarm rate (FAR) [*] and detection efficiency of the network. Other internal parameters, such as the black pixel probability, the coincidence window etc., have been set in order to have neglegible impact on the final FAR and detection efficiency.

3.2. Background and detection efficiency estimation

The background is estimated by applying the pipeline to 4000 resamplings of the network data sets with a total live-time of 2760 days. Each resampling is obtained by applying a rigid time shift to the data of the Virgo detector, ranging from -2123s to +2123s in steps of ≈ 1 s. These shifted data sets should be a good statistical sample to estimate the background of the observation, since they preserve the main characteristics of the original data sets and cancel out the effect of any foreground or signal.

The detection efficiency has been computed over a number of different waveforms (mainly elliptically polarized damped sinusoids) by means of software injections, i.e. by overposing simulated signals on the real data sets, with a mean rate of one per minute. We have generated sets of 994 simulated signal templates with central frequency f_0 ranging within the bar bandwidth (850-950 Hz) and decay time τ spanning at most a

¶ The geometric significance is defined as $\sqrt{z_{AU} \times z_V}$ where z_{AU} and z_V are the significances of the two detectors (see eq.s 10 and 11 in [19])
[+] Between Virgo and AURIGA, the light travel time is ≤ 0.8 ms and the phase shift is ≤ 0.5 ms; to be conservative we set the relative time slide to $|t'| < 1.5$ ms.
[*] i.e. the ratio between the number of accidental coincidences and the joint observation time
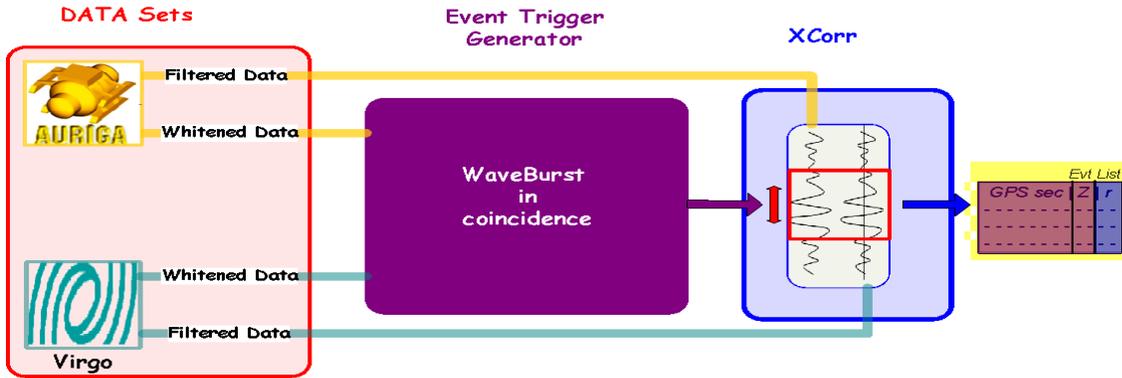
Figure 2: Block diagram of the pipeline. The two detectors whitened data sets are passed to WaveBurst that produces a list of coincident triggers, each characterized by the geometrical significance, Z. The XCorr takes the two weighted filtered data chuncks around the coincident trigger times and slides them looking for the maximum of the cross-correlation coefficient, r.

few tens of milliseconds, with random wave polarization and source inclination with respect to the line of sight. For each template set we have simulated three source populations: sources at the Galactic Center, sources uniformly ditributed in the sky and sources distributed in the Milky Way according to the galactic mass distribution [22]. As usually done in other searches, the signals have been injected for a grid of amplitude values and the detection efficiency has been estimated dividing the number of detected events by the number of the injected signals.

3.3. Tuning of the analysis

The aim of the tuning phase is to optimize the pipeline parameters in order to achieve a low FAR, while preserving the detection efficiency. To avoid any bias on the final results, the tuning phase has been performed on dedicated tuning data sets. In particular we randomly selected half of the time shifted data sets for the background and used dedicated sets of 994 templates of software injections for the detection efficiency. Once the tuning has been completed and the parameters of the analysis have been frozen, we used the other half of the time shifted data and independent sets of 994 injections (estimation sets) to draw the final results. We decided to target the tuning of the analysis to a FAR of $\sim 2/yr$, which correspond to 7 accidental events in the tuning set of time shifted data. Given this small event number, the target FAR can be determined with a statistical sigma of almost 40% and for this reason we decided not to tune to smaller FAR values. We have not applied the Virgo list of vetoes, as from tests performed on the tuning set of the shifts, we measured a $\approx 30\%$ FAR reduction only, while losing 14.5% of the live time. Among the internal parameters of the analysis to be tuned, the cross-correlation window is the most important. The final threshold is set on a linear combination of Z and r.

Cross-correlation Window The general view is that a short time window may be unsuitable for a long signal, as a significant part of its power may be cut off by the window itself. At the same time, if the integration time span is too large, the signal may be diluted in it. Indeed, the weighted cross-correlation filter induces a correlation between the 2 data series over a time scale of the order $\simeq 30$ms. Therefore, even for delta-like signals, we need a cross-correlation window of at least 60 ms. We have set it to 100 ms after testing the performances of various time windows ([25, 50, 100, 200, 400, 800]ms) in terms of FAR and efficiency for narrow and wide band simulated signals.

Combined threshold The selection of candidate events has been achieved by setting a combined (Z, r) threshold on the event list selected by the pipeline instead of considering separate thresholds on Z and r, as previously done [6]. In fig.3, we show an example of how a population of injected signals (dots) detected by the pipeline is distributed for two waveforms. Fig.4 shows the distribution of accidental events. The dashed line shows the optimized combined threshold on (Z,r): such threshold is defined by a simple linear equation: Z=m r + q, where the parameters m and q are chosen to maximize the overall efficiency of the tested source populations and templates at our target FAR. Thanks to the stationarity of the AURIGA performance, the optimal threshold found should be considered as representative of longer joint observations as well.
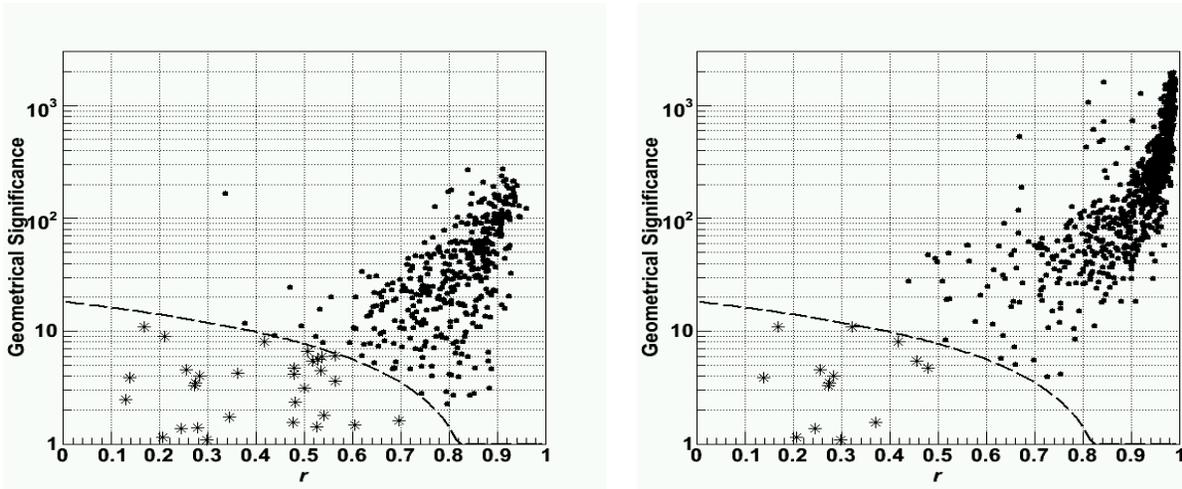

Figure 3: Geometrical significance versus *r-statistic* for two injected Damped Sinusoids (dots). a): DS $f = 914$ Hz, $\tau = 1$ ms, $h_{rss} = 1 \times 10^{-19}$ $1/\sqrt{\text{Hz}}$. b): DS $f = 930$ Hz, $\tau = 30$ ms, $h_{rss} = 1 \times 10^{-19}$ $1/\sqrt{\text{Hz}}$. Asterisks are injected events not passing the threshold (dashed line).

4. Results

The tuned analysis has been applied to the independent sets of time shifted resamples and signal simulations to get the effective FAR and detection efficiency. The resulting
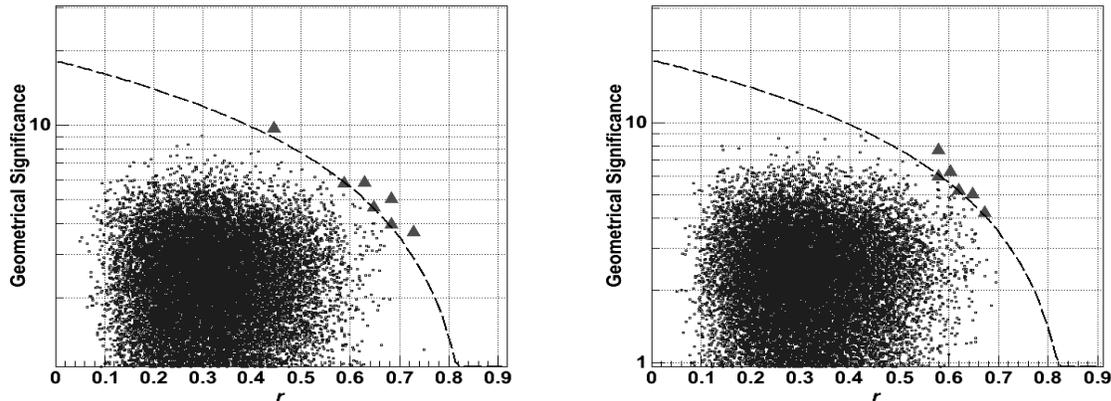
Figure 4: Geometrical significance versus *r-statistic* for background events. a) Distribution of background events of the tuning set. The threshold parameters have been tuned using this set of data in order to reach the FAR of $\simeq 2/\mathrm{yr}$. The accidental events overcoming the threshold are plotted as triangles. b) Distribution of background events of the independent estimation set. The number of events above threshold is 6, leading to a FAR compatible with the result of the tuning set.

FAR is 1.6/yr with a statistical sigma of 0.6/yr (see fig.4b). The detection efficiency of our network is shown in fig.5a, for the 3 injected source populations of damped sinusoids waveforms. The 50% network detection efficiency is achieved in the range $h_{rss}^{50\%} \in [\ 3 \times 10^{-20},\ 1.3 \times 10^{-19}]1/\sqrt{\mathrm{Hz}}\ \sharp$. The detection efficiency depends only slightly on the source populations, while it is strongly affected by the signal duration, as expected due to the AURIGA narrower bandwidth. In fact, the hrss 50% and hrss90% increase by a factor 4.5 and 3 respectively as the signal duration decreases from 30ms to 1ms while, changing the population, the relative variations are within 40%. The h_{rss} is converted into energy emitted in GWs at Galactic Center, assuming a source at distance r from the Earth emitting an infinitesimal energy dE through the element of surface $dA = r^2 d\Omega$ and over the frequency df . By integrating the energy over frequencies and angle $d\Omega$, following eqs.B3 to B6 in [14], we get the conversion into solar masses

4.1. Comparison with the time-frequency coincidence pipeline

We have compared the results of this analysis (i.e. detection efficiency, FAR, observation time) with those of a simpler search based on time-frequency coincidence among triggers detected in AURIGA and Virgo data sets separately. In the simpler search, we have analysed the two data streams separately using WaveBurst as event trigger generator and we searched for coincidences between triggers within a time window $\Delta t = \pm 64\ \mathrm{ms}$ and a frequency window $\Delta f = \pm 25\ \mathrm{Hz}$. We have then applied the list of vetoes for Virgo

♯ The gravitational wave amplitude at Earth, not projected onto the detector arms vectors, h_{rss}, is defined as $h_{rss} = \sqrt{\int_0^\infty (|h_+(t)|^2 + |h_\times(t)|^2)dt}$
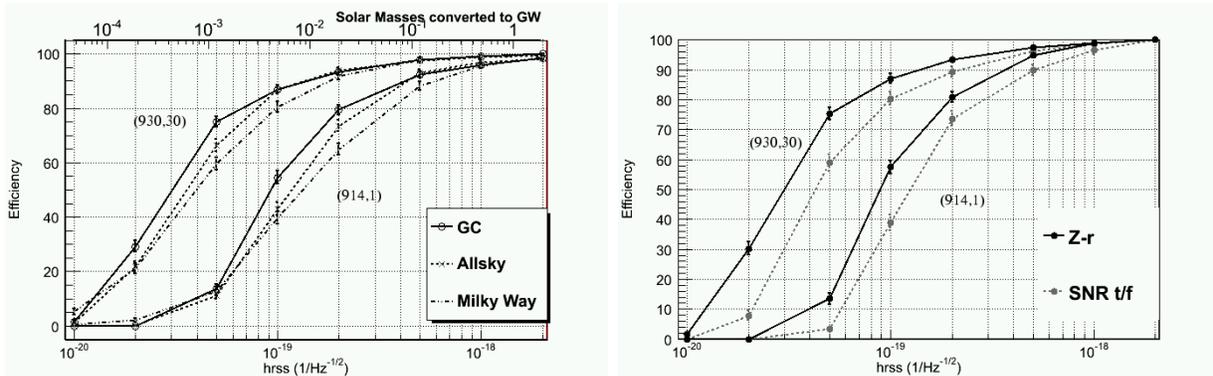
Figure 5: a): Detection efficiencies of the WaveBurst+XCorr pipeline vs h_{rss} for Galactic Center, all sky and Milky Way source populations and for two signals templates (930 `Hz`, 30`ms` and 914 `Hz`, 1`ms`). On the upper x-axis, the h_{rss} is converted to energy emitted in GWs at the distance of the Galactic Center, using eqs.B3 to B6 in [14]. The network response is comparable for the 3 populations while it strongly depends on the signal duration. b): Comparison between the detection efficiencies for the 2 pipelines at FAR $\simeq 2/$`yr`. Solid line: WaveBurst+XCorr pipeline with a combined threshold on (`Z`,`r`). Dashed line: time-frequency coincidence search with two separate thresholds on the `SNR` of the detectors. For the time-frequency search only, the Virgo vetoes were necessary to achieve the target FAR, while preserving a reasonable efficiency. Instead, the WaveBurst+XCorr search results to be robust enough to reduce the FAR also in presence of the extra noise associated to the vetoed time periods. The plotted efficiencies have been normalized to the corresponding live-times, accounting for the 14.5% loss due to the vetoes.

C7 data to the surviving triggers, reducing by a factor ≈ 5 the accidental coincidences at the cost of 14.5% of live time. Finally, separate thresholds on the `SNR` of AURIGA and Virgo have been applied. The threshold optimization has been performed as for the coherent pipeline on the tuning data sets, by setting the same target FAR ~ 2 `/yr` and maximizing the overall detection efficiency over the simulated signals. The best efficiency has been achieved by setting the threshold at `SNR` > 5.6 for AURIGA and `SNR` > 14.5 for Virgo. On the estimation sets, the FAR results $5.3 \pm 1.3/$`yr` and the corresponding detection efficiencies are reported on in fig.5.b for a Galactic Center source population. At similar FAR, the proposed pipeline outperforms the time-frequency coincidence for the tested waveforms in detection efficiency.

5. Conclusions

We investigated the performances of a joint search for GW bursts by a narrow-band resonant detector and a wide-band interferometer using one day of data taken by AURIGA and Virgo in September 2005. The data analysis method based on cross-correlation outperforms a simpler time-frequency coincidence search: it achieves better efficiencies at equal false alarm rate, mostly because it imposes more stringent conditions and better rejects accidental coincidences.

The proposed coherent search shows a 50% efficiency for galactic sources emitting $\approx 7 \times 10^{-4} \div 7 \times 10^{-3} M_\odot c^2$ in GW bursts of $30 \div 1$ ms decay time, provided that their strongest Fourier components are in the AURIGA bandwidth. The resulting detection efficiency of the hybrid network is limited by the less sensitive detector, AURIGA, to $5 \div 10$ times larger amplitudes with respect to a Virgo only search on a larger C7 data set [24] for pulses of $\sim$ 1ms duration. On the other hand, there is a clear advantage of this hybrid search in the background reduction with respect to a single detector search, as it allows to identify candidate events with high statistical confidence.

The main limitations of this methodological study is due to the short duration of the data set used, which prevented us from investigating false alarm rates lower than a few per year. We expect that the efficiency of this methodology would take only very little benefit from the achieved progresses in sensitivity of the interferometric detectors Virgo, LIGO and GEO-600, since the detection efficiency is dominated here by the AURIGA detector. However, these progresses should help reducing significantly the false alarm rate of this search. Further studies with newer and longer data sets are necessary to assess quantitatively this issue. Nevertheless, this hybrid network search could be of interest for the near future, when only one interferometer will be taking data, a likely condition for a large fraction of the time due to the planned instrumental upgrades towards enhanced detectors.

References

[1] See for instance `www.lsc.org` and the talk "Status of LIGO and GEO" by M.Evans available at the Gravitational Wave Data Analysis Workshop 12 web site http://gwdaw12.mit.edu/program.html.
[2] Allen Z *et al.* 2000 *Physical Review Letters* **85** 5046–5050
[3] Astone P *et al.* 2003 *Phys. Rev. D* **68** 022001
[4] Astone P *et al.* 2007 *Physical Review D* **76** 102001
[5] Abbott B *et al.* 2005 *Physical Review D* **72** 62001
[6] Adhikari R *et al.* 2007 *Classical and Quantum Gravity* **24** 5343–5369
[7] http://www.ligo.org/
[8] http://tamago.mtk.nao.ac.jp/
[9] Abbott B *et al.* 2005 *Physical Review D* **72** 122004
[10] Cadonati L *et al.* 2005 *Classical and Quantum Gravity* **22** S1337–S1347
[11] Poggi S *et al.* 2006 *Journal of Physics: Conference Series* **32** 198–205
[12] Baggio L *et al. submitted to Classical and Quantum Gravity* URL `http://arxiv.org/abs/0710.0497`
[13] Jaranowski P, Krolak A, Schutz B F 1998 *Physical Review D* **58** 063001
[14] Acernese F *et al. submitted to Classical and Quantum Gravity* URL `http://arxiv.org/abs/0710.3752`
[15] Cadonati L 2004 *Classical and Quantum Gravity* **21** S1695
[16] Cadonati L and Márka S 2005 *Classical and Quantum Gravity* **22** S1159–S1167
[17] Abbott R *et al.* (LIGO Scientific Collaboration) 2006 *Classical and Quantum Gravity* **23** S29–S39
[18] Rakhmanov M and Klimenko S 2005 *Classical and Quantum Gravity* **22** S1311–S1320
[19] Klimenko S, Yakushin I, Rakhmanov M and Mitselmakher G 2004 *Classical and Quantum Gravity* **21** S1685
[20] Gürsel Y and Tinto M 1989 *Physical Review D* **40** 3884–3938

[21] Chatterji S, Lazzarini A, Stein L, Sutton P, Searle A and Tinto M 2006 *Physical Review D* **74** 082005
[22] Flynn C, Sommer-Larsen J and Christensen P 1996 *Arxiv preprint astro-ph/9603106*
[23] Ott C, Burrows A, Dessart L and Livne E 2006 *Physical Review Letters* **96** 201102
[24] Virgo Collaboration paper on C7 data, in preparation.